Thermal Plasma-aided chemical looping carbon dioxide dissociation for fuel production from alumina particles

M. M. Sarafraz[1], F. C. Christo[1], N. N. Tran[2], L. Fulcheri[3], V. Hessel[2,4]

[1]School of Engineering, Deakin University, Waurn Ponds Campus, Geelong, Australia.

[2] School of Advanced Materials and Chemical Engineering, University of Adelaide, South Australia.

[3] PSL Research University, MINES Paris Tech., Sophia Antipolis, France.

[4] School of Engineering, Coventry, United Kingdom.

Abstract

In the present article, a new thermal plasma-aided process is proposed and analysed that utilises alumina/aluminium (Al_2O_3/Al) metallic particle pair to dissociate steam (H_2O) and carbon dioxide (CO_2) blend (H_2O: CO_2=1) into synthetic fuel using renewable energy. The proposed system utilises two reactors namely synthetic fuel reactor (SFR) and thermal plasma particle regenerator (TPPR) following the chemical looping gasification principle. In the former, the gas blend reacts with aluminium to produce hydrogen-enriched synthetic fuel and alumina, while in the latter, the alumina is dissociated into oxygen and aluminium via equilibrium thermal plasma. It was identified that the proposed system can offer a self-sustaining factor (SSF) of 0.18, thermodynamic and exergy efficiency of 0.38 and 0.68 with renewable energy share of < 0.5 (without battery storage) and > 0.5 (with battery storage) at photovoltaic capacity ~3 MW. The plausible thermodynamic conditions of 1273 K < T < 1573 under lean oxygen condition and 6373 K < T were identified for SFR and TPPR, respectively at which syngas quality (molar ratio of H_2: CO) > 2.05 was achieved. The case study for hybridisation of the plant (at 10% demand fluctuation for a 1.2 MW_{th} TPPR capacity) with photovoltaic solar energy in Pilbara, Western Australia showed that various PV installation capacities can be utilised to partially and fully meet the thermal plasma energy requirements. It was found that the capacity of PV and battery storage are intertwined and regardless of the demand profile of the TPPR, there is a trade-off trend between the capacity of the battery and installation capacity for the PV panels. The optimum storage capacity of 5-6 MWh and 3-4 MW_e PV capacity together with an AC/DC converter of 2.8 MW_e was calculated for the proposed system. The proposed system offers resiliency against the continuous operation in both

centralised and decentralised (local) arrangements. Based on this proof of concept, the practicalness of the thermal plasma-aided process for remote small-scale applications is discussed by benchmarking how it meets the requirements well known for remote gas-to-liquid compact plants, producing gasoline out of syngas.

Keywords: Fuel production; renewable energy; reduction; solar energy; thermal plasma.

1. Introduction

During the ongoing pandemic started in 2020, and currently, in 2021, an invaluable lesson was learned that how human activities affect the future of the earth and the environment. While global warming was suppressed due to the reduction of emission of greenhouse gases [1], again in the year 2021, the CO_2 emission trend is gradually recovered with the potential to surge up due to the re-activation of industrial energy plants [2], which will result in an increase in the average temperature of the earth over the coming year. According to the Paris agreement and also a report released by Intergovernmental Panel on Climate Change (IPCC) [3], a large portion of carbon dioxide is sourced from the industrial sector and transportation showing that the current pathway of combustion of fossil fuels will not be sustainable [4]. Combustion of fossil fuels releases air pollutants such as NO_x, CO_2 [5], and particulate matter (PM2.5) [6], which results in air pollution, environmental damage and intensification of global warming. Therefore, there is a need to further develop energy production systems together with seeking alternative energy resources such as renewable energy to replace fossil fuels and avoid pollutions associated with their combustion.

Chemical looping technology is one of the sustainable technologies that can be harnessed aiming at producing fuel and/or energy from waste solid and/or gaseous hydrocarbon when coupled with renewable energy [7]. A chemical looping system consists of two reactors namely the metal oxide reduction reactor (fuel reactor) and metal oxidation reactor (air reactor). Fig. 1 represents a schematic diagram of the chemical looping process adapted from literature [8]. A solid metal oxide (M_xO_y) is circulated between reactors which transports oxygen from one reactor to another one. It also transfers thermal energy using sensible heat transfer between reactors helping isothermal conditions to be achieved.

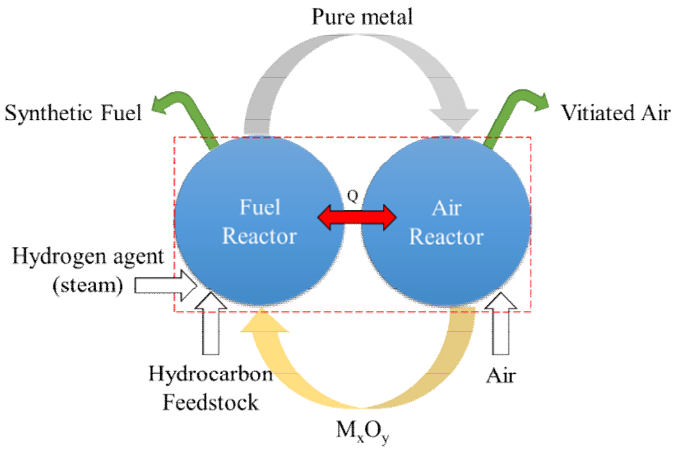

Fig. 1. An illustration of the chemical looping process for synthetic fuel production.

Chemical looping gasification (CLG) is utilised to generate synthetic fuel from waste hydrocarbon [9]. Inside the fuel reactor in the CLG, a hydrocarbon-containing fuel/feedstock reacts with a metal oxide and is oxidised with the oxygen released from the metal particles. Steam is also utilised to enrich the hydrogen content in the fuel reactor and to increase the heating value of the synthetic fuel. Notably, synthetic fuel is a gaseous mixture predominantly consisting of H_2, CO, and CH_4. Furthermore, the reduction of metal and oxidation of feedstock results in the production of fuel and reduces metal particles. The reduced metal particles are then fed into the second reactor to oxidise with air aiming at reproducing the metal oxide. The operation of the system is cyclic, thereby continuously occurring between reactors. Recent studies on chemical looping systems focus on using this technology for energy production via combustion [10], blue, grey, and black hydrogen production via methane reforming [3], bio-derived/hydrocarbon blend gasification [11] and coal [12], respectively. While chemical looping combustion produces CO_2 as a product of combustion, it requires a carbon capture and sequestration (CCS) technology [13] to address the challenges associated with the release of greenhouse gases.

The CCS pathway is to generate energy from fossil fuels while separating carbon dioxide, compressing and storing it out of the process. Currently, the methods developed for CO_2 capture via CLC are oxyfuel combustion, post-combustion, and pre-combustion, which all suffer from low efficiency affecting the economic viability of the CCS. Thus, carbon capture has not been implemented in most of commercial energy plants yet [14]. In the report generated by IPCC [3], it was identified that blue, grey and black hydrogen does contribute to the emission of greenhouse gases, even though all processes target hydrogen as a clean fuel. For blue and grey, the process flow is associated with the emission of CO_2 [15], while in the black route, the carbon from solid feedstock is converted to CO_2 and is released into the atmosphere. Thereby, the production of

hydrogen via methane reforming or gasification of carbon feedstock is only a pathway to transfer carbon from the ground (earth) in form of fossil fuel (natural gas, coal, etc.) to air in form of CO_2. To address the challenges associated with CO_2 production, it is imperative to seek alternative processes that can utilise CO_2 as a feedstock and produce clean fuels using renewable energy resources. By doing so, no further CO_2 is produced and released in the atmosphere, and the current CO_2 will be circulated in the ecosystem until its majority is dissociated using CO_2 to value-added products processes [16].

The dissociation of CO_2 has been extensively studied in the literature. For example, Lindon and Scime [17] have developed a cold plasma reactor (dielectric barrier discharge configuration) to dissociate CO_2 at various operating conditions including various voltage and frequencies. They found that the CO_2 dissociation rate can reach $4 \times 10^{-6}\ mol\ CO_2/s$ with low efficiency of 2.5% at a frequency of 30 kHz over titanium oxide as a photocatalyst [17]. While CO_2 dissociation was experimentally demonstrated, the efficiency and rate of dissociation via cold plasma were very low. In another study, Shang et al. [18] developed a high-capacity thermochemical CO_2-to-CO two-step pathway via iron-poor ferrites in which a variety of iron-poor (Fe-poor, $Fe_yM_{1-y}O_x$) was utilised to produce high-yield CO at a partial pressure ratio of CO: CO_2=1:100. They demonstrated a relative CO yield of 8 ml/g of $Fe_{0.35}Ni_{0.65}O_x$ at the temperature of 1575 K. Recently, Fulcheri et al. [19] assessed potential technologies that can be implemented for dissociating CO_2 and showed that the process of dissociation requires high thermal energy thereby introducing plasma as a potential solution to achieve the thermodynamic conditions required for dissociation reaction. They evaluated different thermal decomposition reactors including thermal plasma, DC corona charge, gliding arc and DBD reactors. By calculating the energy cost of various technologies, they concluded that thermal plasma is a plausible technology that can be utilised to dissociate CO_2 at low energy cost and high yield (LHV basis) providing that electricity is produced via a cheap and clean method such as photovoltaic technology. However, the efficiency of thermal plasma CO_2 dissociation was far from equilibrium (27-43% versus > 99.5%).

In light of the above, the present article is aimed at advancing the knowledge in producing synthetic fuel using a cleaner pathway by developing a new process via chemical looping, thermal plasma and photovoltaic technologies. By utilising renewable energy and also heat recovery blocks, the energy efficiency of the process is maximised, while no CO_2 is produced within the energy blocks of the system.

2. Conceptual modelling

The proposed Chemical Looping CO_2 Dissociation (CLCD) is a plausible pathway and an enabler for employing thermal plasma technology and chemical looping technology to dissociate CO_2 from the air or directly from a chemical/energy plant downstream and convert it into synthetic fuel using a hydrogen agent such as steam. CLCD employs two reactors and a metal oxide particle as an oxygen carrier. The main reactor is referred to as a "synthetic fuel reactor" in which carbon dioxide is dissociated into synthetic fuel in the presence of steam and metal. The metal is oxidised and is then fed into a particle regenerator reactor. The type and configuration of both reactors strongly depend on the type of the material used as metal/metal oxide particles, and also the operating conditions of the reactors. For example, melting temperature of particle, required pressure for the operation of fuel reactor and type of operation (batch or continuous) can affect the selecting procedure for choosing the configuration of both reactors. In the present research, aluminium (Al) and its most stable oxide (Al_2O_3) are chosen as the metallic pair and the oxygen carrier particle. Accordingly, "fluidised bed configuration" for the synthetic fuel reactor and "equilibrium thermal plasma "for the particle regenerator reactor was chosen.

Fig. 2 represents an illustration of the CLCD system developed in this study for producing synthetic fuel from CO_2 driven by renewable energy using an Al/Al_2O_3 oxygen and thermal transport carrier. The synthetic fuel reactor (SFR) is proposed to be a fluidised bed reactor with continuous operation to drive the following reaction:

$$Al(s) + CO_2(g) + H_2O(g) \rightarrow H_2(g) + CO(g) + Al_2O_3(s), \Delta H_{298\,K} = -867\frac{kJ}{m} \qquad (1)$$

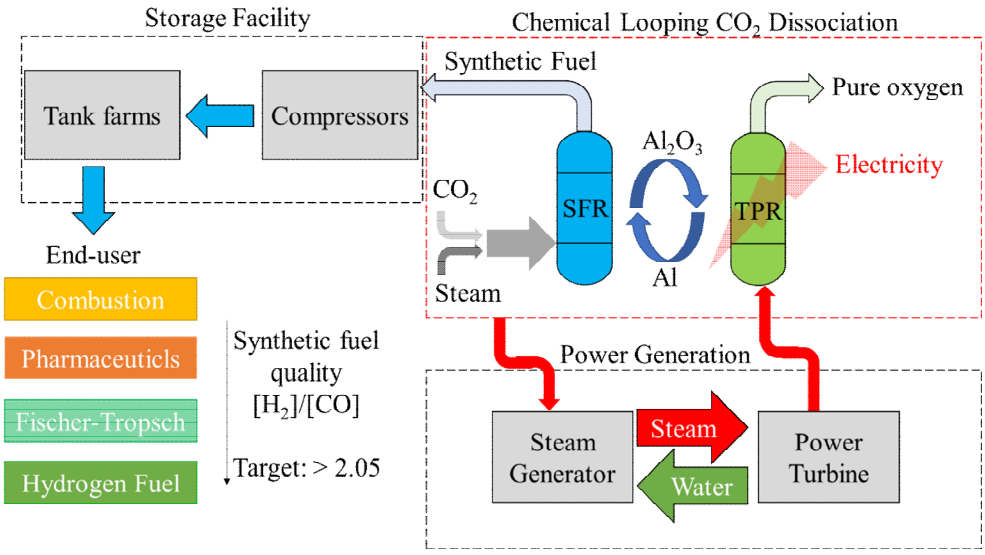

Fig. 2. Schematic diagram of the proposed process developed for synthetic fuel production from carbon dioxide.

The produced aluminium oxide is fed into a thermal plasma particle regenerator (TPPR) in which aluminium oxide is dissociated into oxygen, a useful side production and pure aluminium that is fed into SFR for fuel production, according to the following reaction:

$$Al_2O_3(s) \rightarrow O_2(g) + Al(s), \Delta H_{298\,K} = -1675\,\frac{kJ}{m} \quad (2)$$

Hence, the operation of the proposed system is cyclic following the chemical looping principle. The heat recovered from both SFR and TPPR reactors is utilised to produce high-pressure steam for electricity production. This is to improve the self-sustaining and thermodynamic efficiency of the system, which in turn affects the economic viability and sustainability of the process. The produced fuel will be compressed and stored in a gas facility block next to the developed plant.

3. Reaction thermodynamics and engineering

To evaluate the performance of both reactions, thermochemical equilibrium analysis via the Gibbs minimisation method was utilised [20]. The equilibrium chemical conversion, change in the Gibbs free energy of both reactions 1 and 2, together with enthalpy of reactions and equilibrium constant parameter were calculated and plotted in Fig. 3. As can be seen, reaction 1 occurring in SFR, is thermodynamically feasible to proceed to the equilibrium state regardless of the operating temperature of the reactor. For example, the ΔG value for reaction 1 decreases from -839 kJ/mol at T=300 K to -726 kJ/mol at T=1500 K showing a relatively asymptotic trend around -500 kJ/mol. Hence, the ΔG value remains < 0 regardless of the operating temperature of the reactor. Interestingly, for reaction 2 occurring in TPPR, there is an inflection point at T ~6373 K such that at T < 6373 K, the ΔG value > 0, thereby hindering the dissociation path ($Al_2O_3 \rightarrow Al$) to proceed to the completion. However, at T > 6373 K, the reaction initiated with ΔG= -2 kJ/mol increasing to -144 kJ/mol at T=7000 K. This range of temperature cannot be supplied via conventional reactors. Accordingly, equilibrium thermal plasma such as arc thermal plasma reactors are proposed for this reaction. Overall, in identified thermodynamic temperature conditions for both reactions are plausible offering spontaneous and feasible reactions in the reactors.

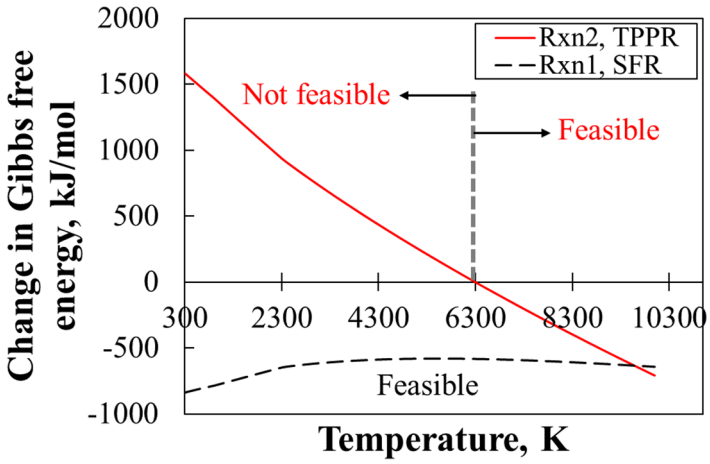

Fig. 3. Variation of change in Gibbs free energy for both reactions with the temperature of SFR.

In Fig. 4, the variation of enthalpy of reaction with the temperature of the SFR is represented. As shown, while reaction 1 in the SFR reactor is exothermic, the alumina dissociation in reactor 2 is highly endothermic, meaning that reaction 1 does not require any external energy resource to maintain the temperature of the SFR reactor. However, a continuous energy line (in this case, electricity) must be supplied to the TPPR to maintain the temperature requirements and driving force for the reactions to proceed to the equilibrium state. Notably, the ΔH value decreased in TPPR by increasing the temperature, for example, decreasing from 1568 kJ/mol at 300 K to 1400 kJ/mol at 4000 K. The same trend was also observed in the SFR reactor meaning that increasing the operating temperature of the reactor decreases the magnitude of the ΔH value. Notably, both reactors experience phase change phenomena (from solid-state to liquid-state) which are technically challenging for fluidised bed reactors and SFR. While for thermal plasma, it is not a technical challenge to drive a phase change embedded reaction regime. Accordingly, it was identified that the upper limit for plausible operating temperature (P.O.T) for SFR reactor is T < 2300 K, while no phase change constraint was identified for TPPR.

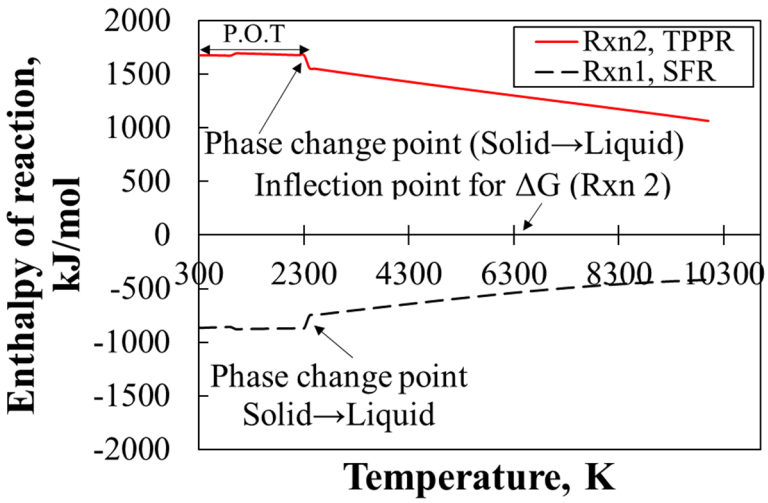

Fig. 4. Variation of enthalpy of reaction for both reactions with the temperature of TPPR.

The sensitivity of the equilibrium constant of both reactions to the temperature of the reactors was also investigated to ensure both reactions can reach the equilibrium state. It is mandatory as a high chemical conversion extent can only be achieved once both reactions have a minimum equilibrium constant > 1. As can be seen in Fig. 5, the equilibrium constants of both reactions reflect a non-linear trend (asymptotic but crossing line x=1) showing that reaction 1 has a very high equilibrium constant at 300 K < T < 1773 K (ΔT~500 K as a temperature buffer was considered to avoid phase change), while for reaction 2, at T > 6373 K, the equilibrium constant becomes greater than 1. These findings are in good agreement with the operating conditions already identified using the Gibbs minimization method in Figs. 3-4.

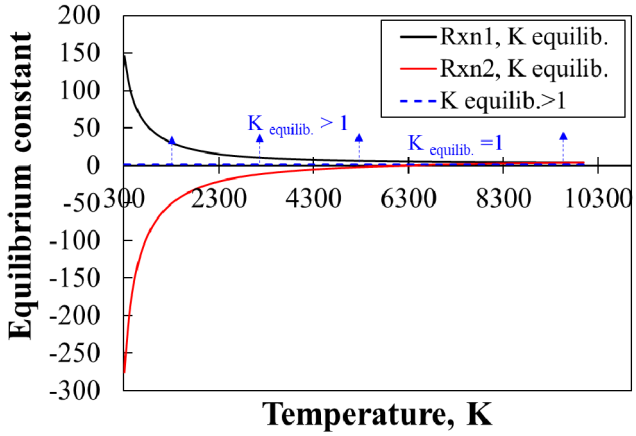

Fig. 5. Dependence of the equilibrium constant of both reactions on the temperature of the system.

To ensure the identified temperature is aligned with the thermochemical equilibrium analysis of the plasma reactor, the Gibbs minimisation method was utilised to identify the equilibrium composition of the outlet from the thermal plasma reactor. In Fig. 6, the results of thermochemical equilibrium analysis for the thermal plasma reactor is shown. As can be seen, a variety of species including Al_2O_3 (solid and gas phases), Al, AlO, N_2 (As a purge gas in the reactor) O(g) and O_2(g) together with charged elements including released electrons and positrons are formed in the thermal plasma reactor. Thus, to obtain pure aluminium from a thermal plasma reactor, the following conditions must be met:

(a) The temperature of the thermal plasma reactor must be higher than 6273 K to ensure the value of the Gibbs free energy is sufficiently high to drive the dissociation reaction ($Al_2O_3 \rightarrow Al$);

(b) A rapid quenching system must be developed with a high heat transfer coefficient, high heat removal rate (high heat flux cooling capacity) and high resistance against erosion and corrosion of metal sublimation. This is because alumina together with pure aluminium exists in the gas phase which can cause severe corrosion in the system;

(c) It is worth mentioning that the current technology readiness level of the thermal plasma reactor has not reached the level that can be utilised for the metal oxide dissociation, however, the capacity of thermal plasma for particle generation from gas reactants has already been demonstrated.

Overall, considering a robust condensation system as part of a thermal plasma reactor, within thermodynamic operating region T > 6273 K, The main species of the reactor are Al, together with oxygen, which is in good agreement with the previous results obtained in Figs 3-5.

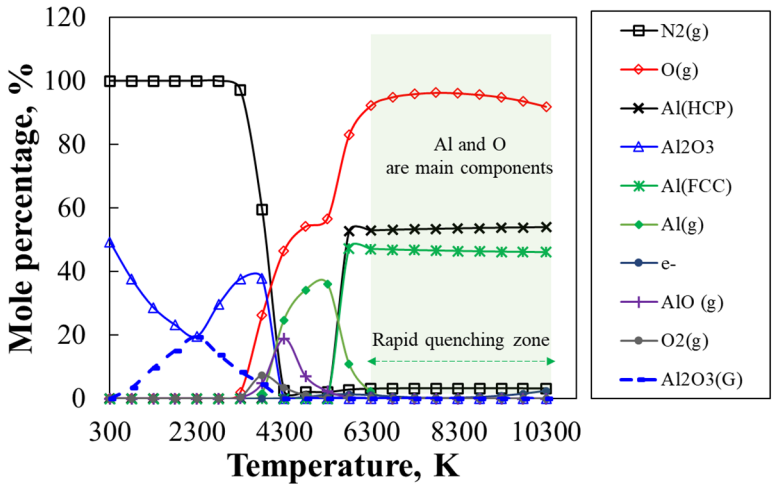

Fig. 6. Variation of the mole fractions of species with temperature in thermal plasma reactor calculated by Gibbs minimisation method under equilibrium thermochemical analysis.

To ensure no carbon particles are deposited on the external surface of the oxygen carrier in the SFR, a thermodynamic analysis was conducted on potential reactions that can generate solid pure carbon inside the reactor. This is because the formation of carbon sedimentation due to sintering or particulate fouling/crystallization can deactivate the reaction sites on oxygen carrier particles resulting in the reduction of performance of the reactors. To investigate this, a thermodynamic equilibrium analysis was conducted to compare the tendency of carbon deposition formation, formation of carbon monoxide and steam carbon dioxide dissociation to identify plausible operating conditions in which carbon deposition is thermodynamically minimised. As represented in Fig. 7, two operating domains were identified based on the variation of $\Delta G/ \Delta G_c$ with the temperature of the reactor. ΔG_c is the Gibbs free energy for the carbon deposition reaction shown in Fig. 7. As shown, for the SFR reactor, at T > 835 K, the Gibbs free energy of carbon deposition reaction is less than hydrogasification and carbon monoxide production reactions showing that the lower temperature limit for the SFR should be T > 835 K to avoid the formation of carbon black and deposition on oxygen carrier particles. Considering a temperature buffer from a lower temperature limit, the SFR reactor can safely operate between 1000 K < T < 1773 K. Overall, reaction thermodynamic analysis showed that the identified operating conditions are plausible for both reactors and also showed that conceptual process design and development within the identified operating condition is feasible.

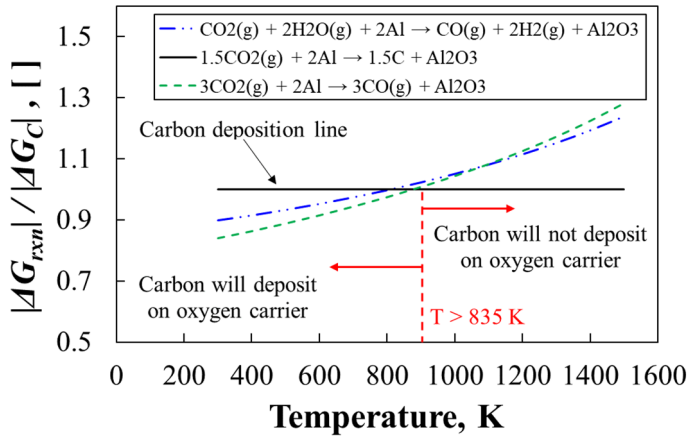

Fig. 7. Comparison between the variation of values of the Gibbs free energy of reactions with temperature in SFR.

4. Process design

An illustration of the proposed process flow diagram is represented in Fig. 8. The process includes three main energy blocks including synthetic fuel and thermal plasma plant (CLCD block), a heat

recovery unit aiming at producing electricity from heat recovered from thermal plasma reactor (power block) and heat exchanging blocks and a storage facility block for compressing and cooling the products (storage block). The synthetic fuel reactor (SFR) is a fluidised bed reactor plausible for solid-gas reaction. In this reactor, direct contact is established between the CO_2-steam gas blend and aluminium particles to generate synthetic fuel. The fluidised bed configuration provides sufficient residence time, relatively good heat and mass transfer for solid-gas reactions [21]. The synthetic fuel produced with SFR is then cooled via a heat exchanger and is fed into a storage facility to be compressed according to the end-user specific requirement. The oxidised alumina particles are then fed into the thermal plasma particle regenerator (TPPR) to regenerate aluminium particles by dissociating alumina into oxygen and alumina. Pure oxygen is another useful product of the proposed plant that can have industrial, and domestic applications. The produced oxygen, if sold on pandemic or post-pandemic markets, particularly under pandemic conditions, can bring tangible benefits to the techno-economic and Levelised Cost of Energy (LCOE) in the process. The regenerated aluminium particles in the TPPR are recirculated to the SFR. While the nature of operation of the proposed system is cyclic, it can be either operated as batch or semi-batch mode depending on the requirements and end-user demands. It is also possible to run the proposed process as a localised plant or a centralised unit under normal and surge conditions.

The heat recovered from TPPR and SFR outlet is utilised to generate steam at 773 K and 60 bar for generating electricity via steam power block. The idea of using heat recovery is to generate electricity to promote the sustainability and self-sustaining characteristics of the thermal plasma plant. In the power block unit, a multi-stage turbine (two-stage, isentropic) is connected to a steam generation unit operated with a high-pressure water line to generate steam via thermal energy recovered from the plant. Hence, the power block does not consume any external energy and any remaining energy after work production is recovered and reintroduced into the steam generation unit. Both oxygen and synthetic fuel are fed into the storage facility unit to be compressed at 35 bar and T=300 K for export and/or storage applications. Accordingly, the storage facility includes two compressors followed by two heat exchangers mounting at the last stage of the compression station to reduce the temperature to 300 K. Table 1 represents the operating conditions and the reference case used for the simulations.

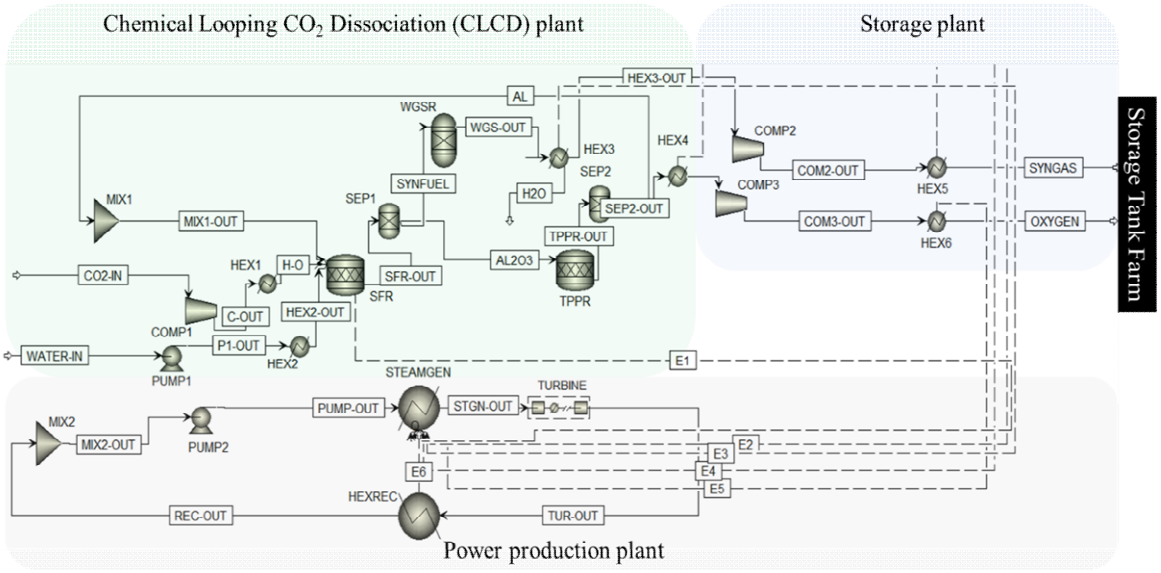

Fig. 8. Schematic diagram of the CLCD process model developed in the present work using Aspen Plus software package.

Table 1. Operating conditions employed for simulating the proposed model.

Operating unit	Value/type	Reference case	Units
Thermodynamic property package*	Uniquac*		-
Compressors			
Isentropic efficiency	0.95	0.95	-
Mechanical efficiency	0.95	0.95	-
Convergent tolerance	0.001	0.001	-
Synthetic Fuel Reactor			
Temperature	1273-1773	1273	K
Pressure	1	1	bar
Thermal Plasma Reactor			
Temperature	6373-6773	6373	K
Pressure	1	1	Bar
Multi-stage turbine			
Number of stages	2	2	-
Discharge pressure	1	1	Bar
Number of coolers	2	-	
Cooler temperature	623 (stage 1) 423 (stage 2)	-	K
Heat exchangers			
Design Pinch point	10	-	K
Heat loss	5	-	%
Pressure drop value	0.2	-	kPa/m

*A series of simulations were conducted with various thermodynamic packages and results were within ±5.5%. The Uniquac model was chosen due to its compatibility with solid-gas, gas-gas reactions, and also hydrocarbon components.

In Table 2, the flowsheet of the simulated process including detailed operating conditions of each stream at reference case is represented system:

Table 2. Flowsheet and operating conditions of each stream in the proposed process modelled with Aspen Plus package at reference condition.

Name	SI Unit	21	AL	AL2O3	C-OUT	CO2-IN	COM2-OUT	COM3-OUT	H2O	H-O	HEX2-OUT	HEX3-OUT	MIX1-OUT	MIX2-OUT	OXYGEN	P1-OUT	PUMP-OUT	REC-OUT	SEP2-OUT	SFR-OUT	STGN-OUT	SYNFUEL	SYNGAS	TPPR-OUT	TUR-OUT	WATER-IN	WGS-OUT
Temp.	K	298	4973	1273	349	298	803	796	298	573	573	298	4973	298	298	298.2	298	298	4973	1273	777	1273	298	4973	423	298	1273
Pres.	bar	1	1	1	2	1	35	35	1	2	2	1	1	1	35	2	60	1	1	1	60	1	35	1	1	1	1
Flow	kmol/h	3.4	10	7.7	2.3	2.3	7.7	3.4	2.9	2.3	8.3	7.7	10	90.6	3.4	8.3	90.6	90.6	3.4	18.3	90.6	10.6	7.7	13.4	90.6	8.3	10.6
Flow	kg/h	109	270	378.9	100	100	88.4	109.1	52	100	150	88.4	270	1632	109.1	150	1632	1632	109.1	520	1632	140.9	88.4	379	1632	150	141
CO_2	kg/h	0	0	0	100	100	27.2	0	0	100	0	27.2	0	0	0	0	0	0	0	0	0	0	27.2	0	0	0	27.2
H_2O	kg/h	0	0	0	0	0	4.4	0	53	0	150	4.4	0	1632	0	150	1632	1632	0	68.1	1632	68.1	4.4	0	1632	150	57
AL	kg/h	0	270	147	0	0	0	0	0	0	0	0	270	0	0	0	0	0	0	147	0	0	0	270	0	0	0
AL_2O_3	kg/h	0	0	231.7	0	0	0	0	0	0	0	0	0	0	0	0	0	0	0	231	0	0	0	0	0	0	0
CO	kg/h	0	0	0	0	0	46.3	0	0	0	0	46.3	0	0	0	0	0	0	0	63.6	0	63.6	46.3	0	0	0	46.3
H_2	kg/h	0	0	0	0	0	10.4	0	0	0	0	10.4	0	0	0	0	0	0	0	9.2	0	9.2	10.4	0	0	0	10.4
CH_4	kg/h	0	0	0	0	0	0	0	0	0	0	0	0	0	0	0	0	0	0	0	0	0	0	0	0	0	0
O_2	kg/h	109	0	0	0	0	0	109.1	0	0	0	0	0	0	109.1	0	0	0	109.1	0	0	0	0	109	0	0	0

Values of stream flow rates were rounded up to numbers with one decimal to fit the whole flow streams in the table. This affected mass balance by ±0.4%.

The thermodynamic modelling was conducted using equilibrium analysis based on the Gibbs minimisation method. To estimate thermodynamic parameters including the Gibbs Free Energy (ΔG) and enthalpy of reaction (ΔH), the following equation was used:

$$\Delta z_{R,i} = \sum_{product\ species} \Delta z_i^f - \sum_{reactant\ species} \Delta z_i^f . \quad (3)$$

where Δz_R is either the Gibbs free energy of reaction (ΔG_R) or can be enthalpy of the reaction (ΔH_R). The subscripts "*i*", refers to species such as CO, H_2, CO_2, CO, CH_4, and H_2O. Likewise, *f* refers to the "formation state" for each thermodynamic property that can be obtained from thermodynamic databases at 298 K. To evaluate the calorific value of the syngas, the following equation was employed:

$$E\chi = \dot{Q}_{syngas} \times (\dot{n}_{H_2} \times LHV_{H_2} + \dot{n}_{CO} \times LHV_{co} + \dot{n}_{CH_4} \times LHV_{cH_4}). \quad (4)$$

Here, $\dot{n}$ is the molar flow rate of the synthetic fuel stream. *LHV* is the lower heating value of the reactive species (~10.1 MJ/kg for CO and ~120 MJ/kg for H_2 and ~50 MJ/kg for CH_4).

The syngas quality (molar ratio of hydrogen to carbon monoxide) was also calculated using the following equation:

$$\varphi = (\frac{\dot{n}_{H_2}}{\dot{n}_{CO}}). \quad (5)$$

Here, $\dot{n}$ is the molar flow rate of hydrogen and/or CO. Also, the combustion quality was defined as:

$$\chi = (\frac{\dot{n}_{CO_2}}{\dot{n}_{CO}}). \quad (6)$$

Here, $\dot{n}$ is the molar flow rate of CO_2 and CO. The total thermodynamic efficiency of the process is defined as follows:

$$\eta_{th} = \frac{\sum_{i=1}^{n} n_i \times \Delta H_i]_{out} - Q_{HEX,p} + W_{power\ block} - W_{pump} - W_{compressor} - Q_{loss}}{\sum Q_{net,R_Z} + \sum_{i=1}^{n} n_i \times \Delta H_i]_{in}}. \quad (7)$$

Where, $W_{power\ block}$ is the calculated work extracted from power block, W_{pump} is the energy requirement of pumps, $W_{compressor}$ is the amount of work consumed by compressors including CO_2 and storage compressors. Likewise, Q_{loss} is an assumed heat loss to the environment, calculated as ~3% of the total energy balance of the plant [22].

Also, the following assumptions were made to simplify the simulations and also to reduce the risk of divergence of the model:

1- There are no side reactions between alloys, reactors, pipes and joints and oxygen carrier particles in the system.

2- Aluminium particles retain their reactive sites over the cyclic operation, and hence, there is no particle-particle interaction in the system. All reactions occur in gas-solid phases.
3- No water is generated inside the turbine and the last stage of the turbine purges the saturated steam at 150 °C and 1 bar. In this condition, the vapour fraction of the steam line is (x=1).
4- Reactions follow equilibrium conditions and proceed to the equilibrium states once thermodynamic conditions are met.
5- Compressors and turbines operate in isentropic conditions.
6- No heat loss occurs from operating units, streams and energy lines to the environment.
7- Aluminium and alumina were considered solid materials during simulation. No phase change phenomena occur inside reactors.
8- Mechanical and driver efficiency of the pumps were 0.65 and 0.7, respectively.
9- A buffer temperature and flow rates of ΔT=20 K and $\Delta \dot{Q}$=0.1 kg/h were considered to calculate the required water flow rate in a steam turbine to achieve $T_{Inlet,\ turbine}$ =500 K.

5. Solar energy profile

In Fig. 9, the Global Horizontal Irradiance (GHI) data together with the sky clearness index are shown for Pilbara, Western Australia based on the NASA Prediction of Worldwide Energy Resource (POWER) database at the centre of Pilbara (Latitude: -21.75, Longitude: 121.75). These data will be implemented in the hybridisation of photovoltaic solar energy with the process aiming at calculating the fraction of renewable energy (solar share). Photovoltaic energy can be utilised to decrease the dependence of the process on the power grid and power block, which will promote the economic viability of thermal plasma technology. Notably, the data are average-based and based on 22 years of data collected from July 1983 to June 2005 for the selected location. From the geographical point of view, Pilbara offers vast coastal plains, good reception of solar radiation together with wind energy. Additionally, the location is close to port offering a plausible opportunity for export/import clean fuels to international end-users such as Japan, India and South Korea.

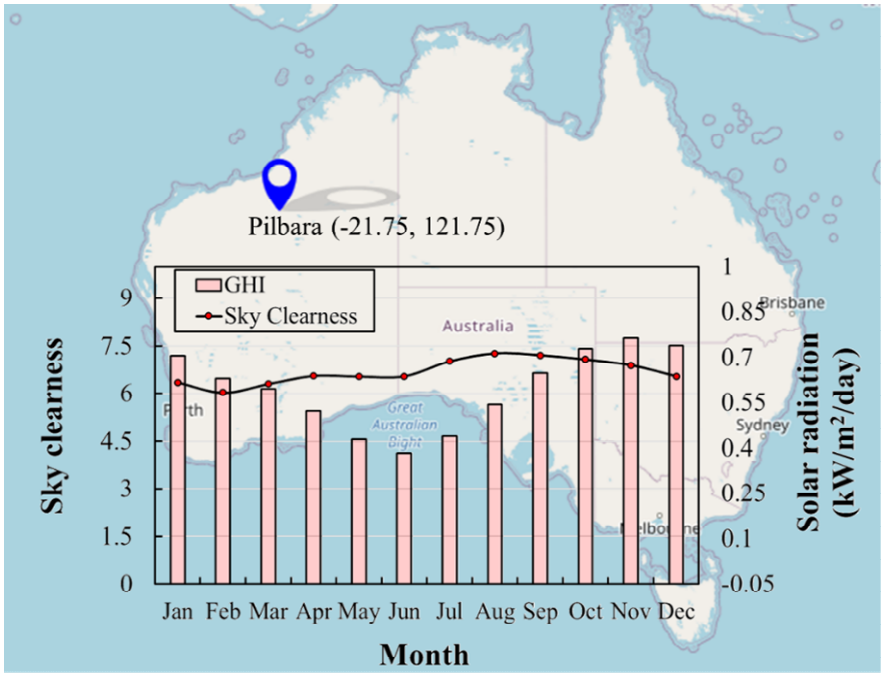

Fig. 9. Global Horizontal irradiance (GHI) and sky clearness parameter for Pilbara, the selected location for the renewable energy assessment.

6. Results and discussion

In the following sections, the effect of various operating parameters on the mole flow of species, syngas quality, efficiency of the plant, and renewable energy fraction are discussed.

6.1.The temperature of synthetic fuel reactor

The variation of the calculated mole fraction of species with the temperature of the synthetic fuel reactor is represented in Fig. 10. Within the operating temperature range of 1273 K < T < 1773 K, with the increase in SFR temperature, a slight change in the mole fraction of species was observed. This shows that the SFR is slightly sensitive to temperature, and thereby, any fluctuation in the spatiotemporal profile of temperature does not affect the outlet of the reactor and the quality of synthetic fuel (φ). This is favourable as the nature of the reactor is exothermic thereby expecting sudden changes in the temperature of the reactor. From 1773 K and higher, the heat transfer paradigm sightly shifts towards a phase change phenomenon (solid-liquid), which can potentially create sintered particles and slag. Sintering and agglomeration clog the reactor and block the particle passages. Accordingly, as discussed, the higher temperature in the SFR reactor must be

avoided to hinder any technical challenges associated with particle sintering, clustering, breakage and agglomeration. The highest hydrogen production rate was observed at 1273 K in which mole flows of species were 5.16 kmol/h (H_2), 1.65 kmol/h (CO), 0.24 kmol/h (H_2O) with 70 ppm CH_4 emission due to the methanation inside SFR.

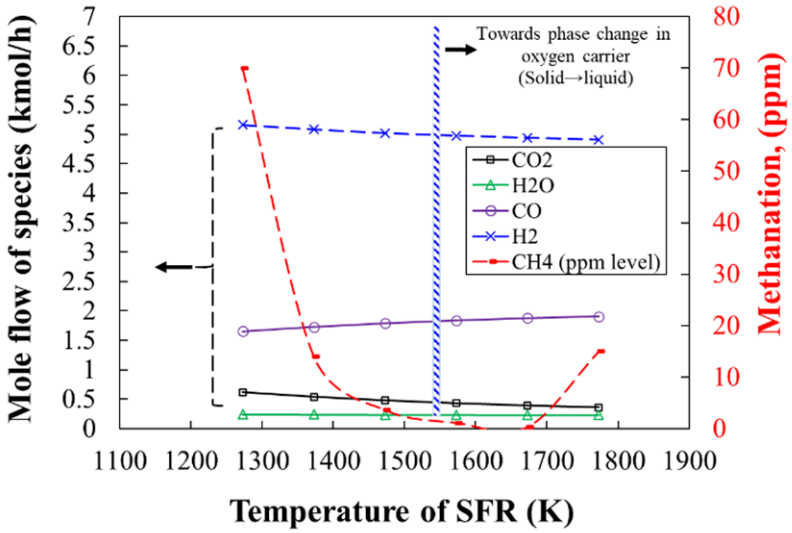

Fig. 10. Variation of mole flow of species with the temperature of synthetic fuel reactor.

6.2.The temperature of thermal plasma particle reactor

Thermal plasma is the key reactor of the proposed process that completes the chemical looping process via regenerating aluminium particles for oxidation reaction with CO_2 in SFR. The thermal plasma reactor operates near-equilibrium conditions, once the minimum temperature requirement is reached. Therefore, the chemical conversion extent reaches the equilibrium value (> 99%) thereby the performance and outlet stream of the reactor are not sensitive to temperature. However, the temperature of the reactor strongly affects the heat recovery and steam production units, thereby influencing the thermodynamic efficiency of the system (η_{th}). In Fig. 11, the variation of the efficiency of the system with the temperature of the TPPR is represented. As shown, at T > 6373 K (where chemical conversion, x > 0.95 in TPPR), the η_{th} =38.2%, together with 26.1% exergy efficiency partitioned in the synthetic fuel offering a plausible combined efficiency of 64.3%. While increasing the temperature slightly increased the efficiency of the plant, it does not affect the syngas exergy efficiency. This is because SFR is the key reactor controlling the chemical performance of the process, while TPPR controls the total thermodynamic efficiency of the process. This means that with an increase in the temperature of TPPR, the thermal energy load in

the steam generation cycle increases thereby producing more electricity. The produced electricity is fed into the thermal plasma which increases the self-sustaining parameter of the plant. At T > 6373 K, the SFF value of 18.4% was achieved meaning that ~18% of the total required energy for a thermal plasma plant can be supplied via the power cycle embedded in the process.

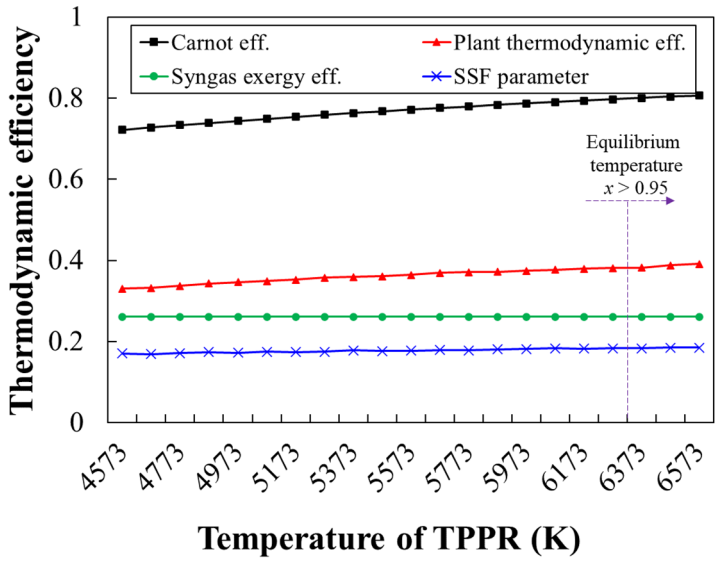

Fig. 11. Variation of Carnot, thermodynamic and exergy efficiency of the process with temperature.

6.3.Quality of synthetic fuel

The quality of synthetic fuel determines its application in industrial and domestic sectors. The higher the quality of the synthetic fuel, the cleaner the application of the synthetic fuel. As represented in Fig. 12, the syngas quality varies with the temperature of the SFR reactor such that by increasing the temperature, hydrogasification reaction which is an endothermic reaction, proceeds towards the equilibrium state. However, partial CO_2 dissociation (shown in Fig. 7) is also an endothermic reaction that produces 3 moles of CO per mole of CO_2, which changes the H_2-CO balance. By increasing the CO content, the syngas quality decreases. For example, at T=1273 K, the syngas quality is ~3.12 decreasing to 2.57 at T=1773 K. For $\varphi > 2.05$, the generated syngas can have clean applications such as liquid fuel production and Fischer-Tropsch applications. It is worth mentioning that there is a trade-off between the rate of CO_2 dissociation and the φ value. While φ can be as high as 3.5, the unreacted CO_2 appears in the synthetic fuel line which can potentially limit its applications. Also, it was identified that the yield of hydrogen is a weak function of the temperature of SFR. Accordingly, to achieve the best energetic

performance in the SFR, its temperature must be regulated at T ~ 1273 K in which the highest syngas quality and syngas yield can be achieved.

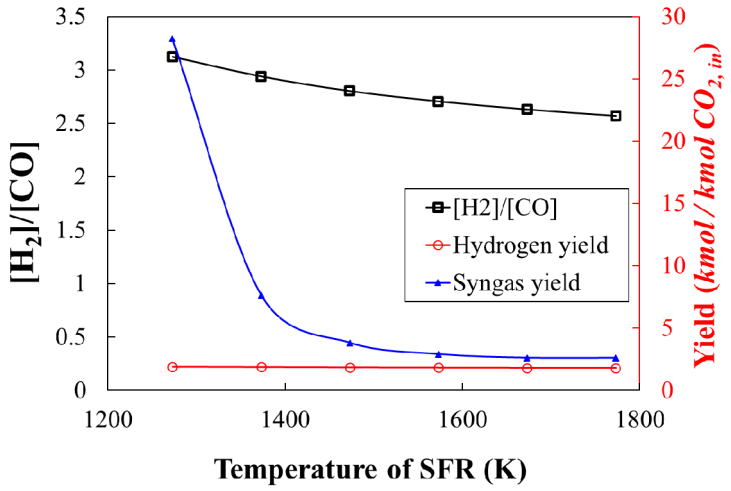

Fig. 12. Variation of syngas quality and syngas yield with the temperature of synthetic fuel reactor.

6.4.Role of water gas shift reactor

The produced synthetic fuel carries high content of CO from partial dissociation reaction, thereby a water-gas shift reactor was utilised to convert part of CO into hydrogen at cost of producing CO_2, but to increase the calorific value and quality of the synthetic fuel. A shown in Fig. 13, the variation of the syngas quality, and syngas calorific value with the temperature of SFR is shown for two case studies one with a water-gas shift reactor and one without it. This is aimed at reflecting the importance of the water-gas shift reactor on controlling syngas quality and its lower heating value (LHV). As can be seen, with an increase in the temperature of SFR, for both scenarios, the φ value decreases. However, φ for the case with WGSR is 16.4% higher (At T=1273 K, up to 18.3% at T=1673 K) in comparison with the value calculated for the process without WGSR. This is associated with the increase in the production rate of H_2 via reacting CO and unreacted steam in the synthetic fuel line. While WGSR is a favourable option to increase the quality of fuel, it can adversely affect the economic viability and techno-economic assessment of the system, which is beyond the scope of the present investigation.

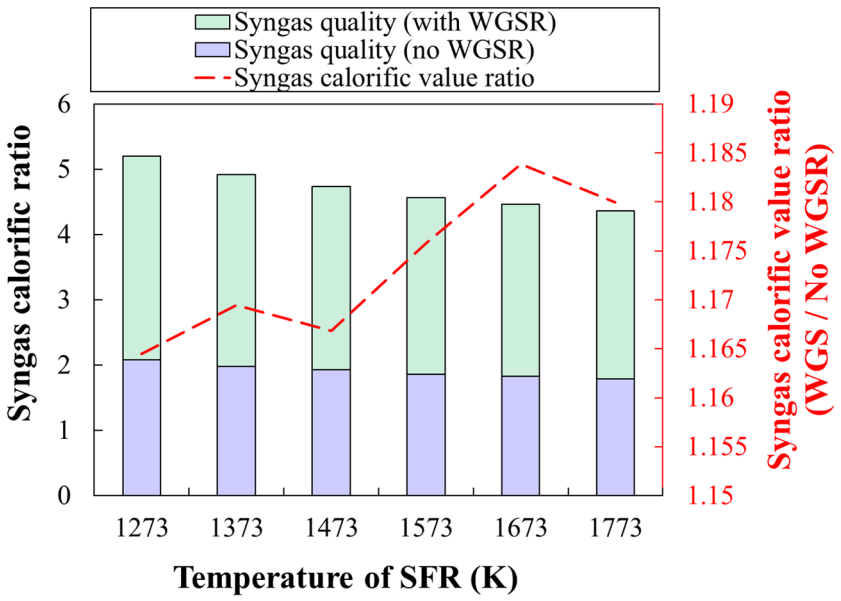

Fig. 13. Variation of the syngas calorific ratio with the temperature of SFR.

6.5.Energy breakdown of the proposed system

In Fig. 14, the energy flow breakdown of the proposed system (either produced or consumed in operating units) assessed at the reference operating condition is depicted based on the energy demand of each operating unit. The plotted chart provides a clear observation of the energy flow of the process, which will help to identify the most plausible target for hybridisation with renewable energy. As can be seen, the water gas shift reactor owns a very small portion of energy flow in the system, while the thermal plasma particle regenerator reactor, followed by steam generation cycle and synthetic fuel reactor has the largest energy demand in the system. The high energy demand of the thermal plasma is associated with the low conversion of electricity to thermal energy and also the thermodynamic operating temperature requirements for dissociating alumina in the TPPR ($T > 6373$ K). As can be observed, the electricity produced by the power block can either be consumed by pumps and compressors or can be dedicated to the TPPR unit. Notably, TPPR consumes 30% of the energy in the system, however, the heat recovery system compensates for 24% of the waste thermal energy from the plant. Likewise, pumps and compressors utilize a very small portion of energy (0.1%) which can be covered by the electricity generated in the power block or independent photovoltaic panels.

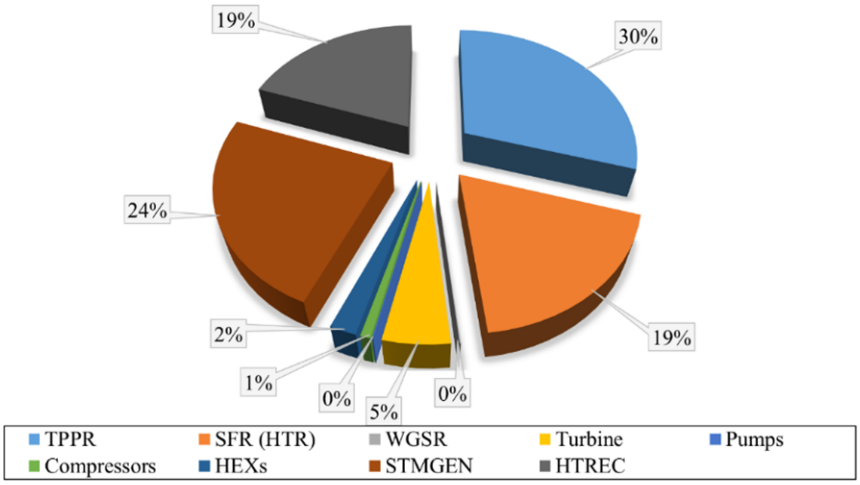

Fig. 14. Energy breakdown of the process against operating units and heat recovery block.

6.6.Hybridization with renewable energy scenario

To harness solar photovoltaic as clean renewable energy, a hybridization strategy must be developed which includes using a smart decision-making microgrid controller, an independent fuel-based utility power block, an AC/DC converter, battery storage together with PV modules. This controlling strategy (shown in Fig. 15) is a key to efficiently utilizing the electricity produced by photovoltaic panels, a power block (with a capacity of 2.1 MW_{th}) and a power grid.

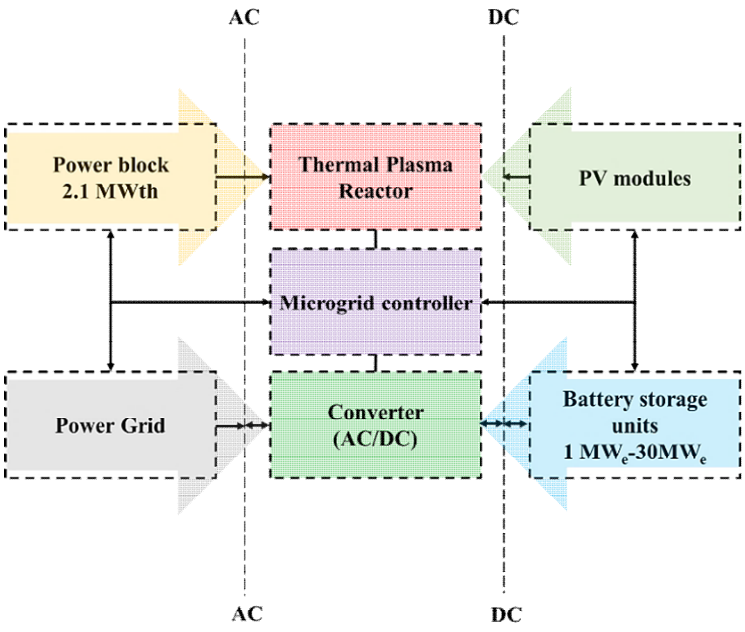

Fig. 15. Illustration of the hybrid system designed for utilizing photovoltaic energy, battery storage, grid and internal power block proposed for the system.

The energy produced from the power block is directly fed into the AC line to be consumed by the TPPR reactor. The electricity produced by PV panels is injected into the DC line and depending on the demand and energy loading profile of the TPPR, the microgrid controller decides to select the most available and appropriate energy resource. For the microgrid controller, a design spec was defined to maximize the renewable energy penetration into the system and to cut the dependence on the power grid and power block. Also, the AC/DC converter module was also controlled by the microgrid by converting DC electricity produced from PV panels into AC when required by the microgrid controller. During peak times (on-sun), the excess electricity produced by solar panels can be stored in the battery storage and can be used during off-sun when solar energy is not available. Once, battery capacity is below 10%, the use of the power grid ramps up reaching the point that can follow the demand profile of the TPPR.

6.7.Energy loading profile analysis

The hourly-based demand profile of the TPPR was calculated from the simulations developed by the Aspen Plus software package. A 10% fluctuation in demand profile due to parasitic losses and energy waste was considered in the simulations. As already mentioned, Pilbara was selected as a plausible location in Western Australia which has a relatively good reception of solar energy (see section 5). The demand-time energy map of the thermal plasma reactor is represented in Fig. 16a. As shown, the scaled demand data are distributed across 8766 hours equivalent to one operating year. According to the distribution plot shown in Fig. 16b, around 54% of demand data are simulated under normal and surge operating conditions showing the ability of the proposed process to be employed as a centralised or localised plant. For a local plant, the normal operating mode is the most plausible scenario, while for the centralised plant, the energy surge is the operating mode. Based on the data analysis, the system can operate under both conditions showing its flexibility against demand. Accordingly, both cases were considered in the energetic performance assessment of the proposed system. The monthly trend of the TPPR is also represented in Fig. 16c showing how scaled energy demand of the TPPR can fluctuate across months of a year. This is vital to understand how the demand of the reactor changes during high-solar (summer) and low-solar (winter) seasons. For low-solar seasons such as April to May, utilization of high-capacity battery storage can be a solution to compensate for the reduced time in which solar energy is available for electricity production.

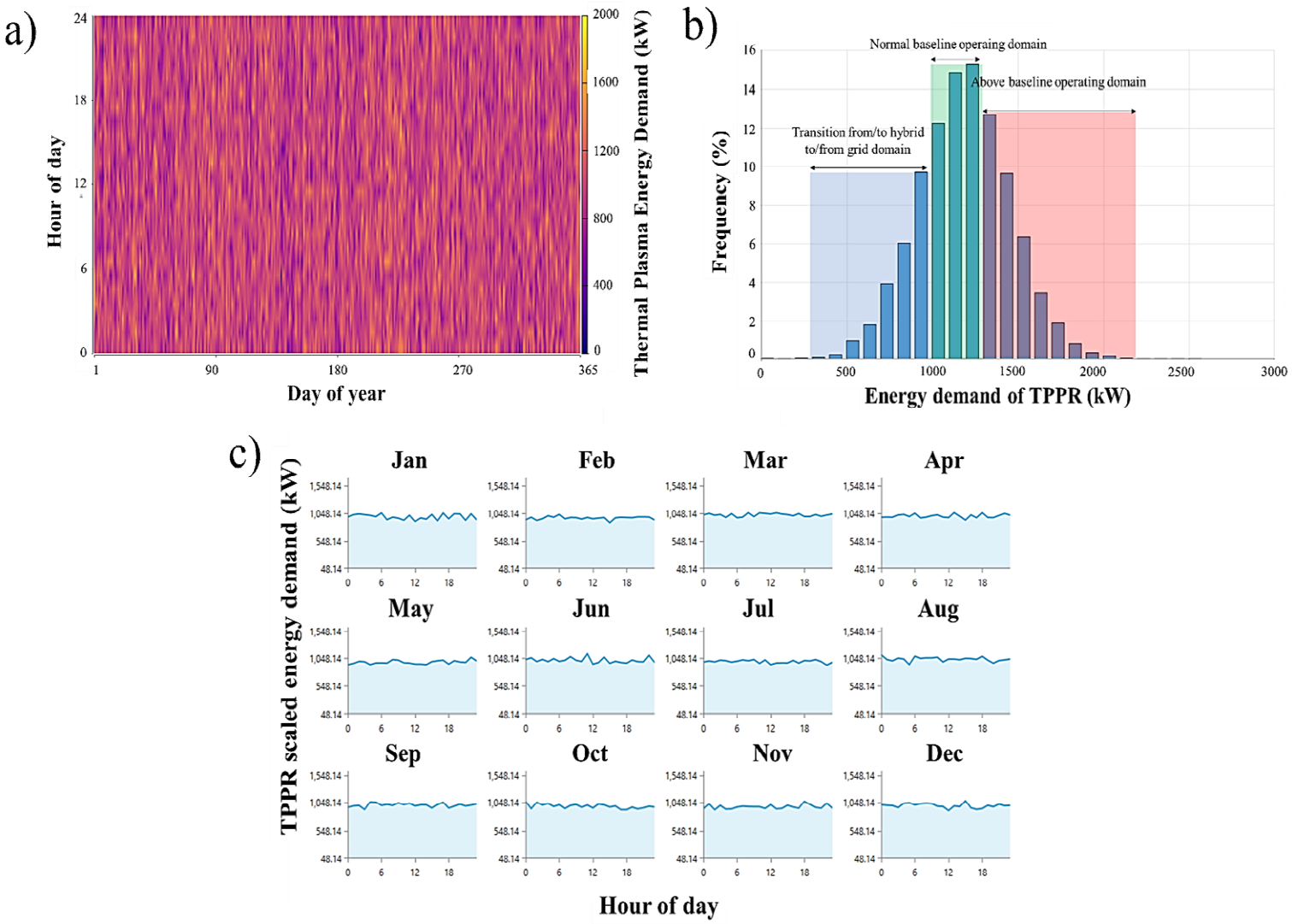

Fig. 16. a) Hourly variation of thermal plasma demand across a year, b) Energy demand fluctuation during normal and surge operating conditions.

In Fig. 17, the variation of the renewable energy fraction with installed PV capacity is depicted. As shown, with an increase in the production capacity of the photovoltaic solar system, the renewable energy fraction of the proposed system increases asymptotically reaching > 50% renewable energy fraction at the capacity of ~3 MW and higher, providing that at least 5 MWh storage battery is installed at the reference case (TPPR capacity= 1.2 MW_{th}). For example, at a production capacity of 1 MW, the system can go 39.9% renewable energy fraction reaching 55% at capacity production 5 MW. Also, a sensitivity analysis was conducted to measure the renewable energy fraction at a PV production capacity of 2 MW, 3 MW, and 4 MW showing that increasing the battery capacity at each PV production capacity can increase the renewable energy fraction

(See Fig. 18 as well). Notably, the installation of 5 MWh battery storage (Li-ion technology) can increase the LCOE value resulting in the suppression of the economic viability of the system. However, by improving the technology readiness level, such capacity can be achievable in a near future. For any PV capacity > 3 MW, the renewable energy is higher than 50% which is a reasonably good solar share considering the intermittent behaviour of solar energy.

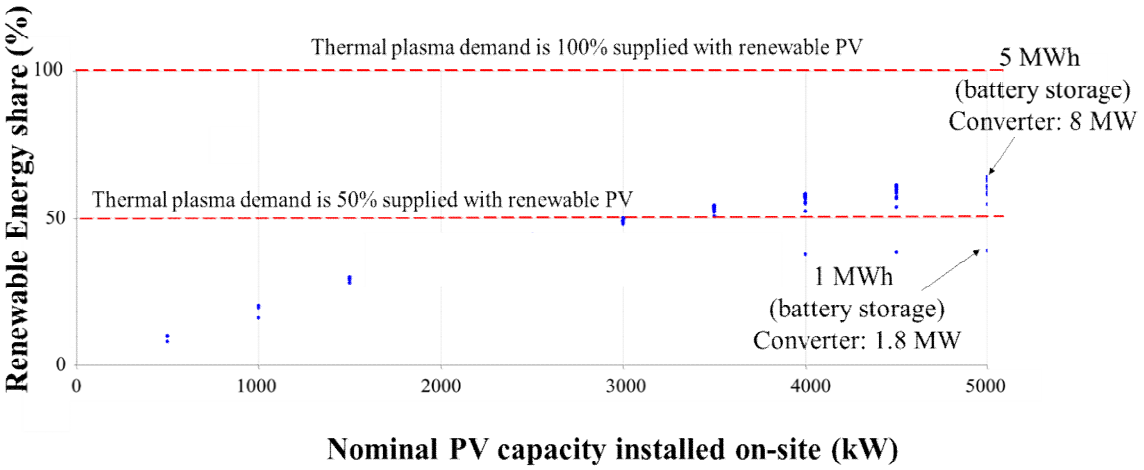

Fig. 17. Effect of PV capacity installed for thermal plasma plant on renewable energy share of the system.

In Fig. 18, variation of the renewable energy fraction and excess electricity production against PV production capacity, and the number of battery storage units is depicted. Each battery represents 1 MWh storage according to the current commercial batteries available in the renewable energy market. As can be seen, with 2 MW PV capacity and a 5 MWh battery storage, the system can go with > 40% renewable energy, which can be increased to 90.9% when battery storage is enlarged to 23 MWh and PV capacity is increased to ~ 5MW. Also, a trade-off trend was identified between the capacity of the battery storage, the capacity of PV installation capacity such that by increasing the PV installation capacity, lower battery storage capacity is required to achieve the same renewable energy fraction. For example, at PV installation capacity of 4 MW and battery storage of 6 MWh, ~68.87% of the system's demand is supplied with renewable energy, however, by reducing PV capacity to 3.5 MW and increasing the battery storage to 16 MWh, the same fraction of renewable energy was obtained. Therefore, it can be concluded that techno-economic conditions together with the technology readiness level of the Li-ion batteries and PV efficiency value will determine the final levelised cost of energy, storage and PV installation capacities.

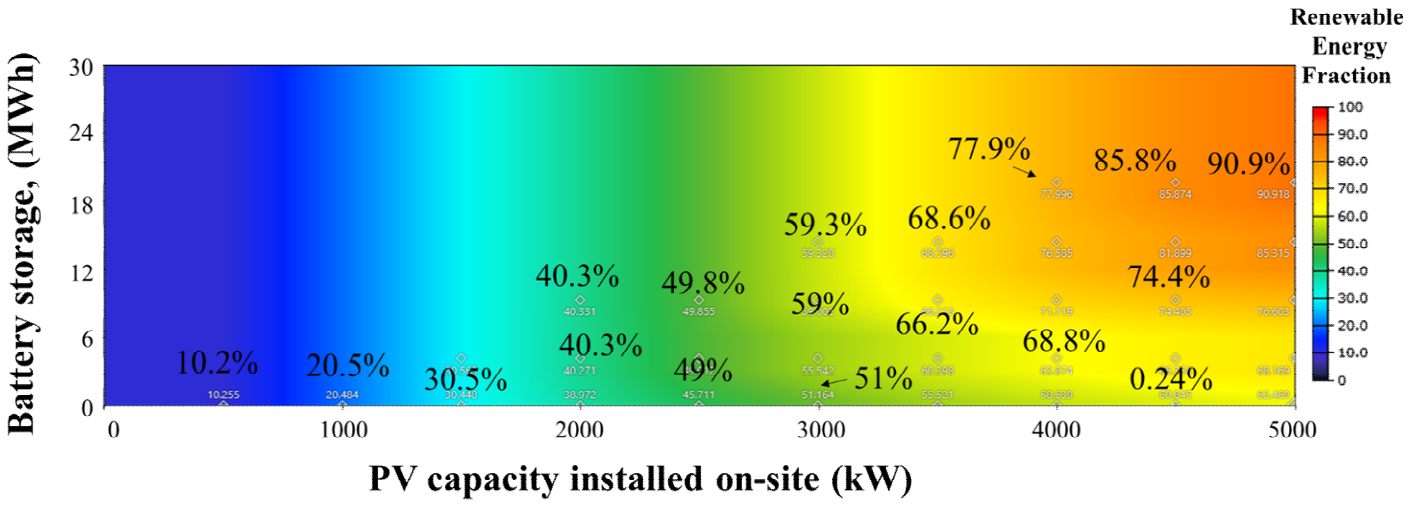

Fig. 18. Effect of battery and PV capacity on renewable energy share of the proposed system.

Overall, this case study revealed that the proposed thermal plasma-aided plant is compatible with renewable energy providing that a techno-economic analysis is conducted on performance-cost characteristics of the proposed system to identify the optimum battery storage and PV installation capacity, which is beyond the scope of the present investigation.

6.8.Future of the technology, technical and economic challenges

Despite plausible features and potentials offered by the proposed system, there is a need to further study to generate technical knowledge required before the process can be harnessed and fully commercialised:

6.8.1. Kinetic studies

While thermodynamic analysis is the first essential step to identify operating conditions and reactor design at the macroscopic level, the micro-scale phenomena such as diffusion and convective mass transfer are key mechanisms affecting the mass transfer coefficient in the reactors. Accordingly, kinetic studies must be conducted to identify activation energy, exponential factor, order of reaction together with mass transfer regimes controlling the reactions inside SFR and TPPR. While this study provides a holistic view and general thermodynamic assessment of the process, it requires further lab-scale and prototype analysis to understand real-life performance and the realistic chemical conversion extent of all reactions.

6.8.2. Particle handling system

Aluminium particles have a relatively plausible density (2.7 g/cm^3) for pneumatic conveyors. While there are commercial conveyors developed for chemical looping systems [23], such systems have not been retrofitted for a thermal plasma-aided chemical looping system. Thereby requiring mechanical studies to identify design specs and key characteristics to develop an efficient particle handling system.

6.8.3. Particle characterisation and analysis in the thermal plasma reactor

TPPR operates at high temperatures and thereby particles are exposed to abrasion, particle breakage, melting point, agglomeration and sintering. The nature of the proposed system is cyclic meaning that particles can be exposed to any of the above corroding phenomena, thereby requiring robust mechanical characteristics and morphology analysis over cyclic operation of Al/Al_2O_3 particles. Hence, a series of surface analysis tests such as SEM, BET, XRD and XPS together with TOC is required to ensure that no carbon is deposited on the external surface of particles and reaction sites remain active over the cyclic operation of the system.

6.8.4. Thermal plasma electrodes

Deposition of metallic particles on thermal plasma electrodes and formation of particulate/crystallisation fouling of metallic micro-particles on thermal plasma can decrease the efficiency of this reactor and can potentially cause reactor failure. This requires further assessment and analysis. Crystallisation fouling reactions and kinetics must be developed and the hindering regime must be identified to avoid damages to the plasma reactor.

6.9.Business opportunities by local processing

6.9.1. Centralised vs. decentralised production models

Small-scale modular units add to the opportunities in industrial chemical processing [24], and plasma operation as process intensification method is generally considered to suit small-scale processing [25-27]. The fertilizer production, for example, can show the pros and cons of producing by central mega-plants or in distributed, local fashion to the markets alternatively [25-27]. Local production may avoid delay due to lead time, reduce emissions, lower transportation costs, and may better access to surrounding renewable energy sources such as solar, wind, and biomass, etc. A local production may also allow a greater integration/use of renewable feedstocks (i.e. biomass); resulting in a more sustainable process and possibly with greater amounts of CO_2 credits [28]. We have given a life cycle assessment for potential scenarios of distributed small-

scale fertiliser processes to identify the best operating conditions in which environment and process economy are balanced; also hypothesising a circular production concept based on biomass [25-27]. Furthermore, we have shown the economic viability of the regional regional production concept recently for thermal plasma-based ammonia fertilizer production [29]. A regional plant is considered as intermediate capacity between local and world-scale production, such as 100 kt/a for a bulk-scale chemical. This demonstrates that new process technologies can be disruptive enough to potentially break the economy of scale (Moore's law); at least to a part.

The thermal plasma process in this paper may suit regional and likely local production; the latter is taken in the following. As syngas is its product and this can be favorably turned into liquid synthetic fuel, such as gasoline for usage in combustion vehicles. That would be typically done on an industrial scale by the Fischer-Tropsch process which produces hydrocarbons from carbon monoxide and hydrogen (syngas). This constitutes a major gas-to-liquid process (GTL). Thermal plasma processes, as presented in this paper, might be particularly effective to integrate into such small-capacity GTL applications on a local scale, denoting processes from possibly 10 kt/a to 100 kt/a. Indeed, learning can be drawn from small-scale GTL [30-32], which aim to produce transportable liquid products from remote smaller natural gas reservoirs, since they cannot be profitably connected to pipeline infrastructure. Yet, one major point needs to be accentuated. The design of small-scale GTL processes is inherently different from that of large-scale GTL counterparts, being originally conceptualised for large-scale production, which creates challenges for a considerable redesign on the local scale. On the contrary, we expect that thermal plasma processes operate best at a relatively smaller scale.

In the following and the sense of a qualitative requirements engineering, a scouting benchmarking is attempted how the here proposed thermal plasma process meets the requirements of local GTL processing such as small, remote gas reservoirs. These process- and economic requirements are well-known and well documented in the literature [32-34].

Utilities: Access to basic utilities such as water, electricity, and sewage disposal is limited at remote sites. Thus, the fewer utilities one process technology needs (and in fewer amounts), the better it is for remote operation. The thermal plasma process proposed here needs electrical energy on-site for the operation of the thermal plasma plant, which can be supplied with stand-alone technologies such as concentrated photovoltaic and photovoltaic systems. By integrating battery storage (e.g. 15 MWh), the intermittent behaviour of solar energy can be addressed and the self-sustaining factor of the process is improved.

Pressurised operations will need compressors as an expensive capital utility that are costly to operate and that have a large utility footprint. For the proposed thermal plasma process, the whole plasma process plant operates at atmospheric conditions, thereby there are no technical challenges associated with pressuring the system. This also eliminates the cost associated with the compressing, pressure regulation and erosion/corrosion due to the high-pressure high-temperature (HPHT) operation.

Gas preconditioning: GTL processes may need pure H_2 (or pure O_2) and this demands a gas purification unit, or similar; making the design complex. The technology typically used, pressure swing adsorption, is complex and costly [35]. The thermal plasma process proposed here is independent of any catalysts, adsorption materials and operates at near-equilibrium conditions meaning that the dissociation reaction of alumina to aluminium can simply proceed to the equilibrium (99% conversion) without producing side chemicals or impurity inside the reactor.

GTL processes often need raw gas (e.g. syngas) conditioning, which involves condensation and recovery of water, separation, and recovery of the raw gas (e.g. of the CO_2), or additional pre-reactions (e.g. water-gas-shift for Fischer-Tropsch). The thermal plasma process proposed here needs a rapid quenching system to be developed for quenching metal vapours to avoid reaction between aluminium and oxygen. The proposed system requires a heat recovery system to cool the outlet oxygen before it can be fed into the storage unit.

Transience: The productive lifetime of the reservoir might be short. That might ask for a relocation of the plant and having its longer operational lifetime taken to multiple uses (and locations). A modular design and compact footprint of the plant would support its mobility; see over the next section. There is also a need for simple site remediation, which again one would expect to scale with the size of the plant, and its need of utilities; giving benefits potentially to the thermal plasma process.

Location: Local factors such as the climate, access to skilled personnel, and legislation play a considerable role in the profit and cash flow of a chemical plant. A modular design can lead to pre-legislation, facilitating the final local legislation. It can also help to increase the process automation requiring less or less skilled personnel. It also favours maintenance as a response to (extreme) climate impacts on the operationality.

Accessibility limitation: The roads leading to the remote location will have a more limited carrying capacity for heavy loads. This limits size and weight of prefabricated equipment. On the contrary, modular equipment with fast assembly and generally equipment at small footprint are

favoured; at best the whole plant is operated on the back of a truck, which has been coined "Chemistry on Wheels" by Evonik Company [36]. The thermal plasma process proposed here is process intensified leading to compact plant size, and it supports the Chemistry on Wheels concept. The process concept of this paper favours modular plant design from standardised units. Currently, the capacity of the metal particle production for the state-of-the-art thermal plasma reactors is low (at bench scale), requiring several units of thermal plasma reactors to operate in parallel to compensate for the low production rate. These reactors can operate independently, with the same performance and conversion rate. This is because thermal plasma operates at very high temperatures, thereby following thermodynamic equilibrium. Hence, depending on the end-users requirements, any number of reactor units can be designed and utilised following "chemistry on wheels" principles to meet the demands.

Flexible feed: The locality of the production site and its specific conditions (geological, climate, etc.) often is accompanied by a range of feed compositions. Some Fischer-Tropsch technologies, for example, do not have that flexibility, which in essence will result in a decreased efficiency of light olefin recovery, which is the wanted outcome. The proposed plasma process is flexible against any feed ratios. Depending on the molar ratio of steam/CO_2, or the flow rate of the metal circulating between reactors, the demand of the thermal plasma plant can be adjusted or the number of reactors can be increased, thereby any configurations at any feed conditions can be designed and implemented.

Process robustness: GTL processes are known to need catalyst exchange or reactivation, which needs human interaction and shutdown of the plant operation [35]. In the proposed thermal plasma plant, there is no need to use any catalytic agent or a catalyst. The reactions proceed towards equilibrium and at T > 6373 K, the chemical conversion of the thermal plasma plant is > 99%.

Environmental control: GTL plants might release emissions, e.g. a sulphur-dioxide-(SO_2)-rich off-gas [35]. That needs to be trapped by additional equipment. While that is standard practice in large-scale plants, it adds a level of complexity at a smaller scale. The expected emissions of the thermal plasma plant are associated with unreacted carbon dioxide that might be sourced from the low performance of the synthetic fuel reactor (SFR). However, a simple recovery system can return the unreacted CO_2 into the feed stream and avoid potential emissions to the environment. Also, the production of carbon is hindered in the process, thereby there is a low risk of producing CO or CO_2 from carbon. Notably, the thermal plasma reactor can operate with 100% renewable energy. Hence, there is no emission expected from the thermal plasma reactor.

Product quality: defines the intended market. Higher product quality will increase the logistical complexity of the operation, yet still, be in the economic incentive range. This has been discussed in the example of olefin oligomerization for Fischer-Tropsch small-scale GTL processes. The product quality of the thermal plasma plant might open oxygen market and aluminium purification market, or if further increased, it can be utilised for other metals such as copper, and iron as well.

7. Conclusion

In the present article, a new process plant was developed based on thermal plasma dissociation of alumina and dissociation of H_2O/CO_2 blend via chemical looping process promoted with thermal plasma technology. The following concluding remarks were drawn:

- Reaction thermodynamic studies showed that both dissociation of CO_2 and alumina are feasible at thermodynamic conditions identified via the Gibbs minimisation method. The temperature range of 1273 K-1773 K for synthetic fuel reactor and T > 6373 K for thermal plasma reactor at atmospheric pressure were selected in which the chemical conversion extent for both reactions approach the equilibrium operating point.
- For the selected thermodynamic conditions, the synthetic fuel quality (H_2: CO molar ratio) was > 2.05 suitable for liquid fuel production, fertiliser and also propulsion and ballistic applications.
- Methanation (emission of methane at vol.% =1 and higher) did not occur in the synthetic fuel, thereby the proposed system had no emission of harmful gases to the environment. The highest CH_4 emission was at 70ppm at 1273 K, which was decreased by increasing the temperature of the SFR.
- The thermodynamic efficiency of the system was ~0.37 far from Carnot efficiency, however, the exergy efficiency partitioned to synthetic fuel was 0.78 which could compensate for the low thermodynamic efficiency calculated for the plant. This was associated with the partitioning of energy in form of chemical exergy storage in the synthetic fuel rather than mechanical work produced by the embedded power block in the plant.
- Thermal plasma had the largest energy consumption rate in the process and thereby, a practical hybridisation strategy with photovoltaic energy was identified as a potential solution to address this technical challenge.

- The installation PV capacity of > 3 MW_e with low battery storage capacity (> 6 MWh) or lower PV production capacity with higher battery storage (e.g., > 15 MWh) were identified as plausible hybridisation characteristics for photovoltaic solar energy. The final decision-making parameter is the technology readiness level of the battery and also the efficiency and technology of the PV panels.

Overall, the thermodynamic potential identified in thermal plasma can be harnessed providing that a renewable resource is hybridised with the system. To achieve this, a robust techno-economic analysis must be conducted aiming at calculating the LCOE for different hybridisation scenarios and for various quality of synthetic fuel to identify the technology-LCOE response curve at various operating conditions.

Finally, the practicalness of the thermal plasma-aided process for bespoke small-scale applications has been discussed. A detailed benchmarking of several main requirements is done, which are taken from well-documented literature for remote gas-to-liquid compact plants, producing gasoline out of syngas. It is shown that the thermal process proposed here meets most of those requirements; possibly in some cases better than typical small-scale (Fischer-Tropsch) processes. The insight of this paper was crucial for making this comparison, and the benchmarking discussion has been structured along with those findings. In this way, we envision the use of the thermal plasma process together with Fischer-Tropsch to make gasoline out of water and carbon dioxide by an integrated two-step process.

Acknowledgement

Mohsen Sarafraz acknowledges the financial support received via the “Vice-Chancellor Alfred Deakin Research Fellowship” program. Mohsen Sarafraz gratefully acknowledges the supports received from the School of Engineering, Deakin University. Volker Hessel and Nam Nghiep Tran acknowledge support from the ERC Grant Surface-COnfined fast modulated Plasma for process and Energy intensification (SCOPE) from the European Commission with Grant No. 810182.

References

[1] X.P. Nguyen, A.T. Hoang, A.I. Ölçer, T.T. Huynh, Record decline in global CO2 emissions prompted by COVID-19 pandemic and its implications on future climate change policies, Energy Sources, Part A: Recovery, Utilization, and Environmental Effects, (2021) 1-4.
[2] K. Santos, L. Delina, Soaring sustainably: Promoting the uptake of sustainable aviation fuels during and post-pandemic, Energy Research & Social Science, 77 (2021) 102074.
[3] R. Carapellucci, L. Giordano, Steam, dry and autothermal methane reforming for hydrogen production: a thermodynamic equilibrium analysis, Journal of Power Sources, 469 (2020) 228391.
[4] O.M. Butt, M.S. Ahmad, H.S. Che, N.A. Rahim, Usage of on-demand oxyhydrogen gas as clean/renewable fuel for combustion applications: a review, International Journal of Green Energy, (2021) 1-25.
[5] I.S. Anufriev, Review of water/steam addition in liquid-fuel combustion systems for NOx reduction: Waste-to-energy trends, Renewable and Sustainable Energy Reviews, 138 (2021) 110665.
[6] P. Maciejczyk, L.-C. Chen, G. Thurston, The Role of Fossil Fuel Combustion Metals in PM2. 5 Air Pollution Health Associations, Atmosphere, 12 (2021) 1086.
[7] A. Joshi, V. Shah, P. Mohapatra, S. Kumar, R.K. Joshi, M. Kathe, L. Qin, A. Tong, L.-S. Fan, Chemical Looping-A Perspective on the Next-Gen Technology for Efficient Fossil Fuel Utilization, Advances in Applied Energy, (2021) 100044.
[8] J. Adanez, A. Abad, F. Garcia-Labiano, P. Gayan, F. Luis, Progress in chemical-looping combustion and reforming technologies, Progress in energy and combustion science, 38 (2012) 215-282.
[9] J. Udomsirichakorn, P.A. Salam, Review of hydrogen-enriched gas production from steam gasification of biomass: the prospect of CaO-based chemical looping gasification, Renewable and sustainable energy reviews, 30 (2014) 565-579.
[10] A. Lyngfelt, Chemical looping combustion: Status and development challenges, Energy & Fuels, 34 (2020) 9077-9093.
[11] X. Zhao, H. Zhou, V.S. Sikarwar, M. Zhao, A.-H.A. Park, P.S. Fennell, L. Shen, L.-S. Fan, Biomass-based chemical looping technologies: the good, the bad and the future, Energy & Environmental Science, 10 (2017) 1885-1910.
[12] Q. Guo, Y. Cheng, Y. Liu, W. Jia, H.-J. Ryu, Coal chemical looping gasification for syngas generation using an iron-based oxygen carrier, Industrial & engineering chemistry research, 53 (2014) 78-86.
[13] J. Godin, W. Liu, S. Ren, C.C. Xu, Advances in Recovery and Utilization of Carbon Dioxide: A Brief Review, Journal of Environmental Chemical Engineering, (2021) 105644.
[14] J. Adánez, A. Abad, T. Mendiara, P. Gayán, L.F. De Diego, F. García-Labiano, Chemical looping combustion of solid fuels, Progress in Energy and Combustion Science, 65 (2018) 6-66.
[15] Z. Navas-Anguita, D. García-Gusano, J. Dufour, D. Iribarren, Revisiting the role of steam methane reforming with CO2 capture and storage for long-term hydrogen production, Science of the total Environment, 771 (2021) 145432.
[16] N. Gutiérrez-Guerra, J.L. Valverde, A. Romero, J.C. Serrano-Ruiz, A. de Lucas-Consuegra, Electrocatalytic conversion of CO2 to added-value chemicals in a high-temperature proton-exchange membrane reactor, Electrochemistry Communications, 81 (2017) 128-131.
[17] M.A. Lindon, E.E. Scime, CO2 dissociation using the Versatile atmospheric dielectric barrier discharge experiment (VADER), Frontiers in Physics, 2 (2014).
[18] S. Zhai, J. Rojas, N. Ahlborg, K. Lim, C.H.M. Cheng, C. Xie, M.F. Toney, I.-H. Jung, W.C. Chueh, A. Majumdar, High-capacity thermochemical CO 2 dissociation using iron-poor ferrites, Energy & Environmental Science, 13 (2020) 592-600.
[19] A. Lebouvier, S.A. Iwarere, P. d'Argenlieu, D. Ramjugernath, L. Fulcheri, Assessment of carbon dioxide dissociation as a new route for syngas production: a comparative review and potential of plasma-based technologies, Energy & fuels, 27 (2013) 2712-2722.
[20] P. Kangas, I. Hannula, P. Koukkari, M. Hupa, Modelling super-equilibrium in biomass gasification with the constrained Gibbs energy method, Fuel, 129 (2014) 86-94.
[21] S. Iannello, S. Morrin, M. Materazzi, Fluidised bed reactors for the thermochemical conversion of biomass and waste, KONA Powder and Particle Journal, 37 (2020) 114-131.

[22] J.S. Goodling, Microchannel heat exchangers: A review, International Society for Optics and Photonics, pp. 66-83.
[23] J.H. Chiu, H.E. Andrus, G.N. Liljedahl, P.R. Thibeault, System for hot solids combustion and gasification, Google Patents, 2012.
[24] T. Seifert, S. Sievers, C. Bramsiepe, G. Schembecker, Small scale, modular and continuous: a new approach in plant design, Chemical Engineering and Processing: Process Intensification, 52 (2012) 140-150.
[25] A. Anastasopoulou, R. Keijzer, B. Patil, J. Lang, G. van Rooij, V. Hessel, Environmental impact assessment of plasma-assisted and conventional ammonia synthesis routes, Journal of Industrial Ecology, 24 (2020) 1171-1185.
[26] A. Anastasopoulou, R. Keijzer, S. Butala, J. Lang, G. Van Rooij, V. Hessel, Eco-efficiency analysis of plasma-assisted nitrogen fixation, Journal of Physics D: Applied Physics, 53 (2020) 234001.
[27] A. Anastasopoulou, S. Butala, B. Patil, J. Suberu, M. Fregene, J. Lang, Q. Wang, V. Hessel, Techno-economic feasibility study of renewable power systems for a small-scale plasma-assisted nitric acid plant in Africa, Processes, 4 (2016) 54.
[28] M.M. Sarafraz, N.N. Tran, H. Nguyen, L. Fulcheri, R. Burton, P. Wadewitz, G. Butler, L. Kirton, V. Hessel, Tri-fold process integration leveraging high-and low-temperature plasmas: From biomass to fertilizers with local energy and for local use, Journal of Advanced Manufacturing and Processing, 3 (2021) e10081.
[29] N.N. Tran, J. Tejada, M. Razi Asrami, A. Srivastava, A. Laad, M. Mihailescu, A. Costa, E. Rebrov, V. Lai, P. Phan, G. Butler, V. Hessel, Economic optimisation of local Australian ammonia production using plasma technologies with green/turquoise hydrogen, ACS Sustainable Chemistry & Engineering, (accepted paper) (2021).
[30] V.S. Arutyunov, V.I. Savchenko, I.V. Sedov, I.G. Fokin, A.V. Nikitin, L.N. Strekova, New concept for small-scale GTL, Chemical Engineering Journal, 282 (2015) 206-212.
[31] Z. He, G. Khatu, E. Tenenbaum, W. Li, Z. Han, Flared Gas Monetization with Modular Gas-to-Liquid Units: Oilfield Conversion of Associated Gas into Petrol at Small-Scales, OnePetro.
[32] O. Ajagbe, R.G. Moghanloo, Small-Scale GTL, A Sustainable Alternative for Production of Transport Fuels in The US, OnePetro.
[33] A. De Klerk, Sasol 2 and 3 facilities, Fischer-Tropsch Refining; Wiley-VCH: Weinheim, Germany, (2011) 181-212.
[34] A. de Klerk, Fischer–Tropsch refining: technology selection to match molecules, Green Chemistry, 10 (2008) 1249-1279.
[35] A. De Klerk, Consider technology implications for small-scale Fischer-Tropsch GTL, Gas Process, (2014) 41-48.
[36] Evonik, Chemistry on Wheels, Evonik Industries, https://corporate.evonik.de/downloads/corporate/2014-22-december-chemistry-on-wheels.pdf, 2014.